A Review of Gold Mineralization in Mali

David M. Lawrence, James S. Lambert-Smith and Peter J. Treloar

Abstract

Economic gold mineralization in Mali is confined to two terranes of Birimian-aged (Paleoproterozoic) rocks in the south and south-west of the country. The West Mali gold belt, along the border with Senegal, hosts two world-class orogenic gold districts (>5 Moz of Au mined or in reserve): the Loulo-Gounkoto and Sadiola-Yatela complexes. This gold province is hosted within greenschist metamorphosed siliciclastic and carbonate sedimentary rocks along the eastern side of the Kédougou-Kéniéba inlier, with mineralization linked to higher-order shears and folds related to the Senegal-Mali Shear Zone. Gold deposits within the West Mali gold belt show many features typical of orogenic gold mineralization, such as geological setting (accretionary orogen), late-orogenic timing (strike-slip deformation; post peak metamorphism), structural paragenesis, and deposit geometry (steep, tabular ore bodies). However, alteration assemblages (tourmalinization, silica-carbonate, sericite-chlorite-biotite, calc-silicate) and ore fluid compositions (carbonic-rich and high-salinity aqueous-rich fluids) are highly variable along the belt. Fluid inclusion and stable isotope studies have shown that this variability is caused by multi-fluid sources, with magmatic, evaporitic and regional metamorphic fluids all likely contributing to gold mineralization within the region. Supergene enrichment of the orogenic gold lodes is economically important in the northern parts of the West Mali gold belt, involving karstification of mineralized limestones. In addition to orogenic gold deposits, other styles of gold mineralization have been reported within the Birimian crust of West Africa. The Morila gold deposit, in southern Mali,

D.M. Lawrence (✉)
Randgold Resources Ltd, Unity Chambers,
Halkett Street, St Helier, Jersey JE2 4WJ, UK
e-mail: David.Lawrence@randgold.com

J.S. Lambert-Smith · P.J. Treloar
School of Natural and Built Environments,
Kingston University, London KT1 2EE, UK

M. Bouabdellah and J.F. Slack (eds.), *Mineral Deposits of North Africa*,
Mineral Resource Reviews, DOI 10.1007/978-3-319-31733-5_13

is classified as a reduced intrusion-related gold system, in which strata-bound Au–As–Sb–Bi–(W–Te) mineralization formed early in the Eburnean orogenic cycle (syn-metamorphic) with spatial and genetic links to syn-orogenic granodiorites and leucogranites.

1 Introduction

Gold mining in Mali has a long and illustrious history, with artisanal workers having exploited the metal since pre-historic times. During the peak of the Malian Empire in the 14th century, alluvial placers along the Falémé River (which now marks the international border with Senegal) were mined extensively. This mining alerted European and Arab rulers to the mineral wealth of the region, and helped develop political, cultural, and trade links between western Sudan (as it was then known) and the rest of the world. Collapse of the Songhai Empire in the late 16th Century ended the region's dominance in the African and world gold trade.

Commercial gold mining in Mali commenced in the 1970s. The first industrial mine, Kalana, was discovered after a large exploration program by Société Nationale de Recherche et d'Exploitation Minière (SONAREM) (Boltrukevitch 1973). In the following decade, a United Nations assisted project known as the Syndicat Or (a joint venture between the Malian government and BRGM) carried out extensive soil geochemical surveys in the southern and western parts of Mali. This project led to the discovery of many of the country's largest gold deposits, including Gara (previously known as Loulo-0), Sadiola, and Syama (Dommanget et al. 1993; Kusnir 1999). In 1991, Mali relaxed its mining codes, which led to renewed foreign interest and began the recent boom in the country. In 2013, Mali exported 64 t of gold, and is currently Africa's third largest gold producer after South Africa and Ghana (Diarra and Holliday 2014).

2 Geological Setting

The geology of Mali is dominated by Neoproterozoic to Paleozoic sedimentary rocks of the Taoudeni basin (Villeneuve and Cornée 1994), which formed during extensional deformation of the West African Craton during the Neoproterozoic (Brooner et al. 1990). Paleoproterozoic (Birimian; 2.2–2.0 Ga) basement rocks crop out from beneath the Taoudeni cover sequences in the Sikasso region of southern Mali, and in two small windows in the semi-arid Kayes region in the southwest, close to the border with Senegal (Kayes and Kédougou--Kéniéba inliers) (Fig. 1a). Gold mineralization in Mali is restricted to these two Birimian terranes that are referred to here as the Mali South Goldfields and West Mali Gold Belt, respectively.

2.1 Mali South Goldfields

Gold mineralization in southern Mali is located within Birimian rocks of the Baoulé-Mossi domain, which also hosts the well-known Ghanaian gold provinces (e.g., Oberthür et al. 1994; Allibone et al. 2002a, b; Berge 2011), as well as gold mineralization throughout Burkina Faso (Klemd and Ott 1997; Klemd et al. 1997; Béziat et al. 2008) and eastern and central Côte d'Ivoire (Coulibaly et al. 2008; Kadio et al. 2010). The Birimian geology of southern Mali comprises three volcanic-sedimentary belts with adjacent sedimentary basins (Fig. 1b). From west to east, these are known as the Yanfolila-Kalana belt, the Bougouni belt, and the Syama belt. The adjacent basins, from west to east, are referred to as the Siguri basin

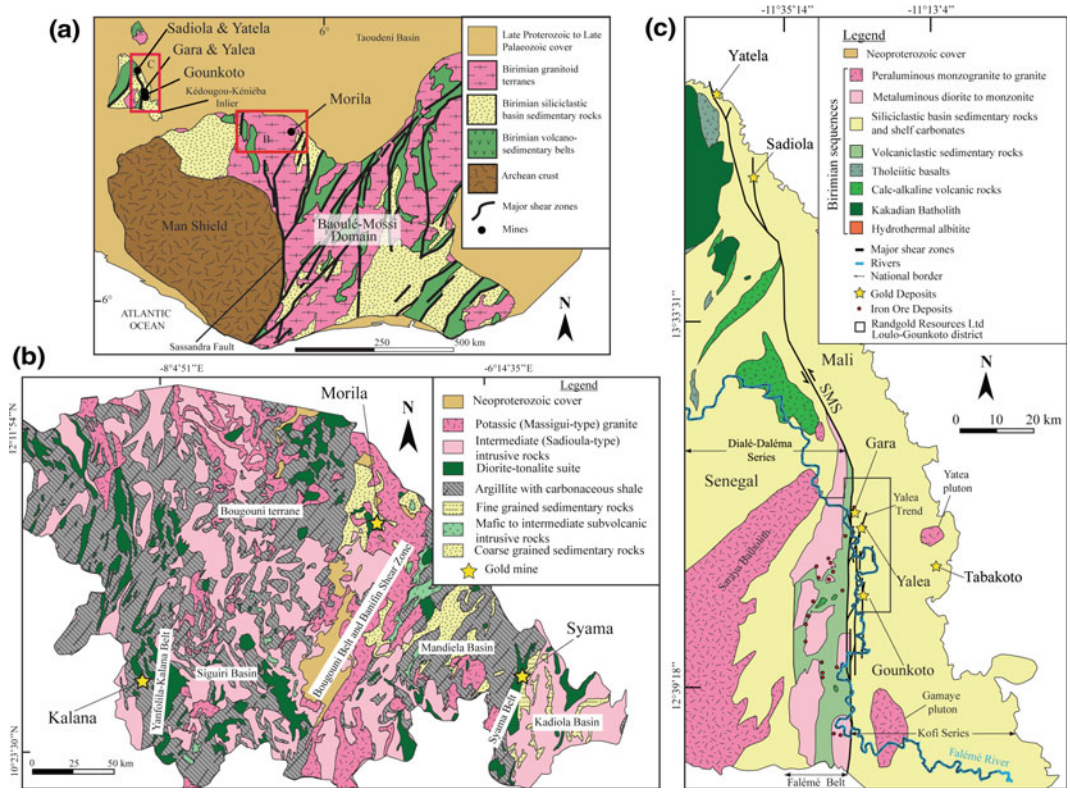

Fig. 1 Regional geologic maps of the Birimian terranes of Mali. **a** *Inset* of West African craton indicating locations of study areas (modified from Feybesse et al. 2006). **b** Detailed map of Mali South Goldfields, showing geology of northwestern part of Baoulé-Mossi domain. **c** Geologic map of eastern (Malian) part of Kédougou-Kéniéba inlier, showing locations of mines within the West Mali Gold Belt (modified from Lawrence et al. 2013a)

(located mainly in Guinea), the Mandiela basin, and the Kadiola basin. This area hosts some major gold deposits, including those exploited at the Morila, Kalana, and Syama mines (Milési et al. 1992; Olson et al. 1992; McFarlane et al. 2011).

Birimian rocks were deformed and metamorphosed during the Eburnean orogeny around 2.1–2.0 Ga. In southern Mali, three Eburnean deformational events have been identified (Liégeois et al. 1991). A first phase of isoclinal deformation (D1) was followed by a D2 phase of NW-SE compression recorded by a widespread, sub-vertical N- to NNE-trending schistosity (S2) and regional greenschist-amphibolite facies metamorphism. Major NNE-trending, sub-vertical, shear structures such as the Baniffin shear zone, which is located 30 km to the east of Morila, formed during a later transcurrent D3 event.

2.2 West Mali Gold Belt

Gold mineralization in western Mali is located along the eastern side of the Birimian Kédougou-Kéniéba inlier (KKI) (Fig. 1c). This inlier straddles the Mali-Senegal border; although the most productive and prospective region lies on the Malian side, and is referred to here as the West Mali Gold Belt. The gold belt extends for approximately 180 km and includes two

world-class gold districts (>10 Moz of Au), the Loulo-Gounkoto complex in the south and the Sadiola-Yatela district in the north, plus the smaller Tabakoto mine and several exploration projects such as the Fekola prospect south of Gounkoto.

The West Mali Gold Belt is hosted within Birimian sedimentary rocks of the Kofi Series (Fig. 1c). The sedimentary basin comprises a thrusted and folded sequence of quartz and feldspar wackes, mudstone, and limestone-marl sequences. In the southern part of the basin, these units are strongly albitized and tourmalinized. Tourmaline-bearing quartz-wackes at Loulo have detrital zircon ages of 2125 ± 27 to 2098 ± 11 Ma (Boher et al. 1992). The Kofi sedimentary rocks are intruded by a series of plutons of various generations and sizes. The largest intrusions are monzogranitic in composition and include the Gamaye pluton in the southern part of the basin, and the Yatea pluton north of the Tabakoto mine. Smaller, calc-alkaline, quartz-feldspar-phyric granodiorite stocks and finer-grained, mafic- to intermediate-composition dikes and sills, cut the sedimentary rocks in both the Loulo-Gounkoto and Sadiola-Yatela districts.

A polycyclic Eburnean deformational history, similar to that recorded in the Mali South Goldfields, is reported for the Kofi Series. The first deformational phase (D1) is a compressive event linked to the initial accretion of the Birimian terranes. D1 deformation is characterized by NNE-to NE-trending recumbent and overturned folds (F1), NW-verging thrusts, and axial planar schistosity (Milési et al. 1989, 1992; Ledru et al. 1991). Later deformation (D2–D3) is associated with transcurrent movement and formation of the regional-scale, N-S, Senegal-Mali Shear Zone (SMS; Bassot and Dommanget 1986). Gold deposits of the West Mali Gold Belt are confined to second- and higher-order structures on the eastern side of the SMS, in which mineralization was synchronous with D3 transtensional deformation (Lawrence et al. 2013a; Masurel et al. in press). Regional greenschist-facies metamorphism and associated plutonism are associated with both compressive and transcurrent phases of deformation. Minor hornblende-hornfels contact metamorphism is seen locally surrounding intrusive stocks at Sadiola.

3 Gold Mineralization Styles

The majority of gold deposits within the Birimian terranes of Mali, and the rest of West Africa, have been classified as orogenic gold mineralization (Milési et al. 1992; Olson et al. 1992; Lawrence et al. 2013a, b). Globally, orogenic gold lodes are shear-hosted deposits that developed along strike-slip fault systems linked to late-stage, non-orthogonal, orogenic crustal growth (Groves et al. 1998, 2000). They form over a range of crustal depths (<6 to >12 km; Groves et al. 1992), although the majority of deposits are hosted in greenschist-facies rocks (Bierlein and Crowe 2000). The general characteristics of orogenic gold deposits are summarized in Groves et al. (1998) and Ridley and Diamond (2000). Recently, a more complex Birimian gold metallogenesis has been recognised, with new styles of gold mineralization documented such as reduced intrusion-related gold systems and gold skarn deposits (McFarlane et al. 2011; Ouattara et al. 2014).

This review documents the genesis of both orogenic gold and reduced intrusion-relation gold mineralization in Mali, with emphasis on the country's four largest ore bodies: Loulo, Gounkoto, Sadiola, and Morila. Discussion of gold mineralization in the West Mali gold belt is a synthesis of three recent studies (Lawrence et al. 2013a, b; Masurel et al. in press). Synopsis of the Morila deposit in southern Mali relies on reports by Hammond et al. (2011) and McFarlane et al. (2011), together with data from two MSc theses by Quick (1999) and King (2012).

4 Orogenic Gold

4.1 Loulo-Gounkoto Complex

The Loulo-Gounkoto complex is one of the largest orogenic gold districts in West Africa. Three main deposits are known: Gara (current reserves of 1.5 Moz at 4.15 g/t), Yalea (reserves of 2.9 Moz at 5.82 g/t), and Gounkoto (reserves of 2.8 Moz at 5.1 g/t) (Randgold Resources Ltd 2014). The Gara ore body was discovered during

regional soil surveys by Syndicat Or in 1981. In 1992, Broken Hill Proprietary (BHP) Minerals entered into an option and share purchase agreement with Syndicat Or, and did work in the Loulo area until 1996 when Randgold Resources Ltd acquired BHP's Malian projects. Randgold carried out an intensive exploration program, which led to the discovery of the Yalea deposit in 1996/1997. In November 2005, the Loulo mine was officially opened. Gounkoto was added to Loulo's resource in 2009, discovered following an airborne electromagnetic survey of the region; mining commenced in 2011, 2 years after initial discovery. The Loulo-Gounkoto complex has produced over 3.5 Moz from both open pit and underground resources, and currently (2015) has a mining lifespan of 9 years at 660 Koz pa.

4.1.1 Yalea

The Yalea ore body is hosted along a third-order shear related to movement along the N-S-trending, brittle-ductile, Senegal-Mali Shear Zone (SMS). The SMS was initiated as a sinistral transpressional fault during the onset of D2 deformation. Higher-order structures that formed during D2 transpression include second-order, NNE-striking sinistral shears (P-shear geometry) such as those in the Yalea Trend. This extends for >20 km from the south of Yalea to the Loulo-2, Loulo-3, and Baboto satellite deposits. The Yalea ore body sits along a 2-km-long, N-S left-hand flexure of the Yalea Trend (known as the Yalea Shear), which formed during transtensional sinistral movement at the start of D3 deformation (Fig. 2).

The Yalea Shear is a 10–40-m-wide zone of strongly altered, brittle- to ductilely deformed rocks that dip 60° to the east at surface and steepen at depth. The footwall consists of argillaceous calcareous sandstone, with hydrothermal-tectonic breccias focused along footwall splays. Hanging-wall lithologies include arkosic arenite grading into arkosic wacke (Fig. 2). A carbonaceous dolomitic limestone caps the ore zone in the south of the deposit. Mineralization consists predominantly of disseminations that are confined to the matrix of hydrothermal and tectonic breccia units along the contact between the argillaceous and arkosic units (Fig. 3).

The alteration halo at Yalea extends 50–100 m into the wall rock and consists of two main components: (1) an early phase of albite-carbonate-quartz alteration that predates the main mineralization event (D2/early D3); and (2) a later syn-mineralization phase of phyllic alteration (D3) (Lawrence et al. 2013a). The first stage of alteration is divided spatially into two zones. An inner texturally destructive zone, located along the Yalea Shear, is carbonate rich and comprises an assemblage of albite-ankerite plus minor quartz, sericite, and pyrite. An outer zone occurs in mylonitic and brecciated footwall lithologies, with alteration becoming less intense and more albite-rich distal from the main shear. Altered zones generally have a pink or orange color due to the presence of fine-grained hematite. Sericite-chlorite alteration overprints the albite-ankerite-quartz alteration along the Yalea Shear. Alteration is confined to narrow (<5 cm) ductile shears, patchy replacements of hanging-wall limestones, interstitial phases in massive sulphide zones, and thin (<3 cm) green to black alteration envelopes surrounding auriferous sulphide stringers and veinlets (Lawrence et al. 2013a).

Disseminated ore assemblages at Yalea are dominated by arsenian pyrite and arsenopyrite, and locally by zones of abundant chalcopyrite. Paragenetic studies reveal a multi-stage ore development (Lawrence et al. 2013a; Fig. 4a). Arsenian pyrite (max. 3 wt% As) forms the first generation of auriferous sulphides and commonly contains euhedral inclusions and intergrowths of fine-grained arsenopyrite. Arsenian pyrite is post-dated by a generation of coarse-grained arsenopyrite that replaces, cuts, and/or forms pseudomorphs of early sulphides. A late phase of cross-cutting chalcopyrite is temporally associated with some gold remobilization. Gold is generally fine-grained (<10 μm); coarser particles up to 50 μm are spatially associated with arsenian pyrite. Gold fineness ranges from 920 to 990 (mean of 950).

4.1.2 Gara

The Gara deposit is 6 km NW of Yalea, adjacent to the Falémé River (Fig. 1c). Mineralization occurs over a strike length of 1.2 km. The

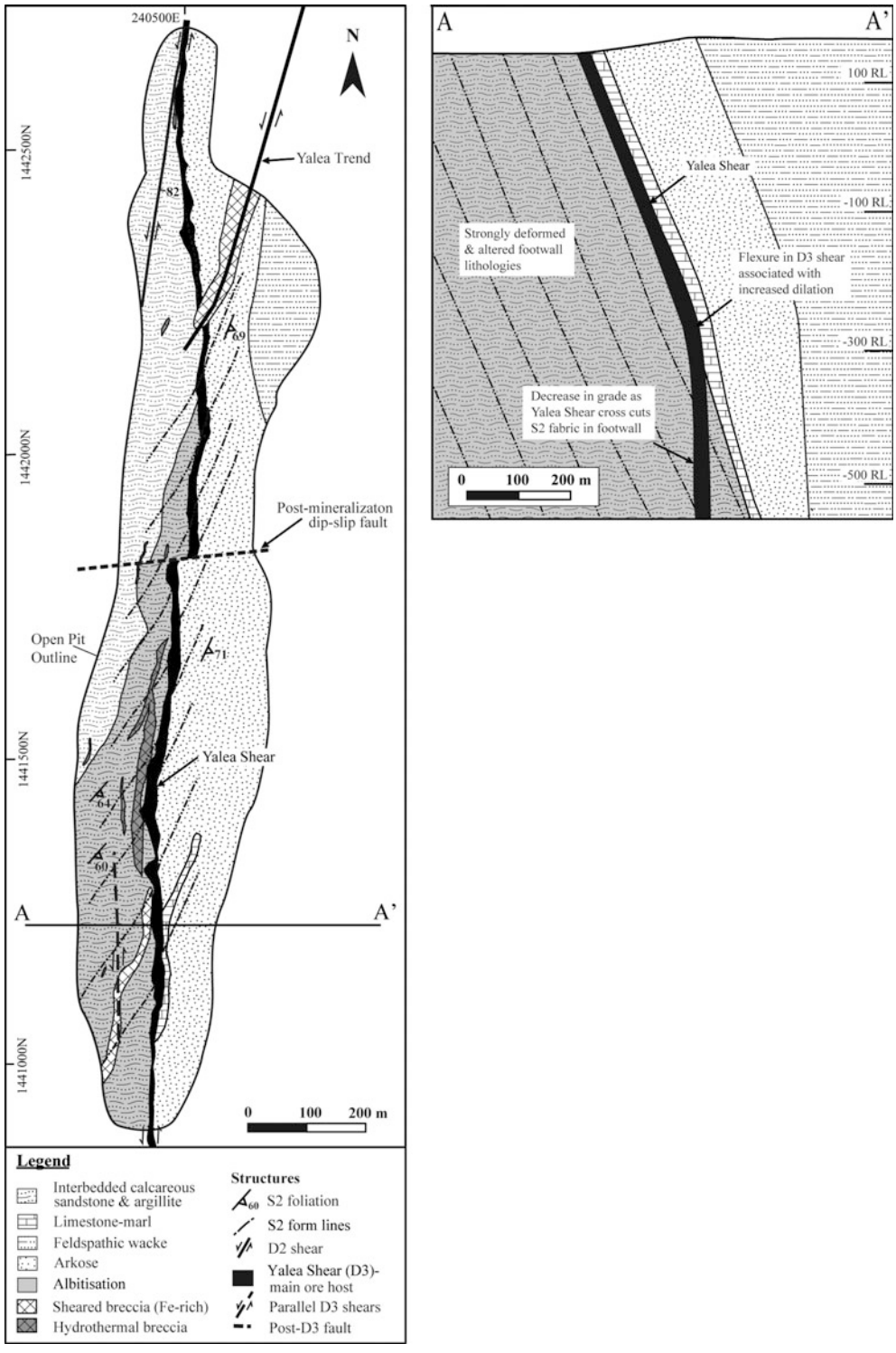

Fig. 2 Geological and structural plan map (*left*) and cross section (*right*) of Yalea gold deposit in Loulo district. Ore body is within a 2-km-long, N-S-trending, D3 structure known as the Yalea Shear, which forms a left-hand flexure in district-scale, NNE-trending, Yalea Trend

Fig. 3 Photograph of brittle-ductile deformation along Yalea Shear with gold mineralization hosted in dark matrix of pink albite-ankerite hydrothermal breccia (Lawrence et al. 2013a)

geometry of the ore body is controlled by macroscopic, SSW-plunging, upright F2 folds, related to transpressive D2 deformation along a series of second-order, NNE-trending shears linked to the SMS (Lawrence et al. 2013a; Fig. 5). Later extensional D3 deformation led to the formation of quartz-ankerite-tourmaline-pyrite-gold shear veins (Fig. 6). Minor amounts of disseminated sulphides surround these veins. The Gara stratigraphy consists of a tourmaline-altered quartz wacke (20–50 m thick), with mineralization being hosted in the most altered "tourmalinite" unit (5–20 m thick). Rocks immediately to the east and west of the ore body consist of carbonaceous limestone and marl, and argillaceous and calcareous sandstone (Fig. 5).

Gara is characterized by intense tourmaline alteration. Early studies at Gara (Milési et al. 1992; Dommanget et al. 1993) suggested that the boron-rich protolith to the tourmalinite had a submarine-exhalative origin. However, Lawrence et al. (2013a) has shown that tourmaline alteration is epigenetic and related to gold mineralization. Tourmaline growth shows a complex, multi-stage paragenesis (Lawrence et al. 2013a). The first generation (early D2) is the most pronounced and forms texturally destructive, cryptocrystalline (<10 μm) tourmaline that pervasively replaces the matrix of the quartz wacke host rock. The second generation of tourmaline growth (early D3) is synchronous with mineralization and forms acicular tourmaline grains (30–50 μm) confined to gold-bearing stockwork veins, commonly aligned perpendicular to vein walls. The last phase of tourmaline alteration (late D3) is a replacement of auriferous pyrite. The first tourmaline alteration event prepared the quartz wacke host for later stockwork vein formation and gold mineralization, by increasing the competency of the rock in relation to the surrounding wall rocks. During D2 and D3 deformations, this unit preferentially fractured, which facilitated fluid ingress (Lawrence et al. 2013a). Early D2 sodic alteration at Gara, analogous to the main alteration at Yalea, albeit with lower carbonate contents, occurs in more distal zones (up to 150 m from the ore body).

In contrast to Yalea, pyrite is the principal sulphide ore mineral at Gara (>95 % of total sulphides). Pyrite forms annealed aggregates and commonly displays minor Ni ± Co substitution (≤ 2 wt% Ni + Co). Trace sulphide assemblages include chalcopyrite, gersdorffite, pentlandite, Ni-bearing pyrrhotite, and arsenopyrite. Monazite, scheelite, and lesser amounts of xenotime are also present. Gold is associated with pyrite (95 %) or occurs as free gold in veins (5 %). Silver concentrations are lower than at Yalea, with gold fineness ranging from 988 to >998 (mean of 994). The ore and alteration paragenesis at Gara is summarized in Fig. 4b.

4.1.3 Gounkoto

The Gounkoto deposit is in the southern part of the mining district, approximately 30 km from Gara (Fig. 1c). The ore body is hosted along a 2-km-long, N-S-trending, third-order, transtensional sinistral structure; elevated grades are spatially associated with left-hand, NNW-trending dilational jogs that formed during late D3 deformation. Mineralogy is characterized by multiple overprinting hydrothermal events (Lawrence et al. 2013a). Strongly sheared semi-pelitic and carbonate rocks show evidence of (from oldest to youngest): (1) early albite-ankerite-quartz

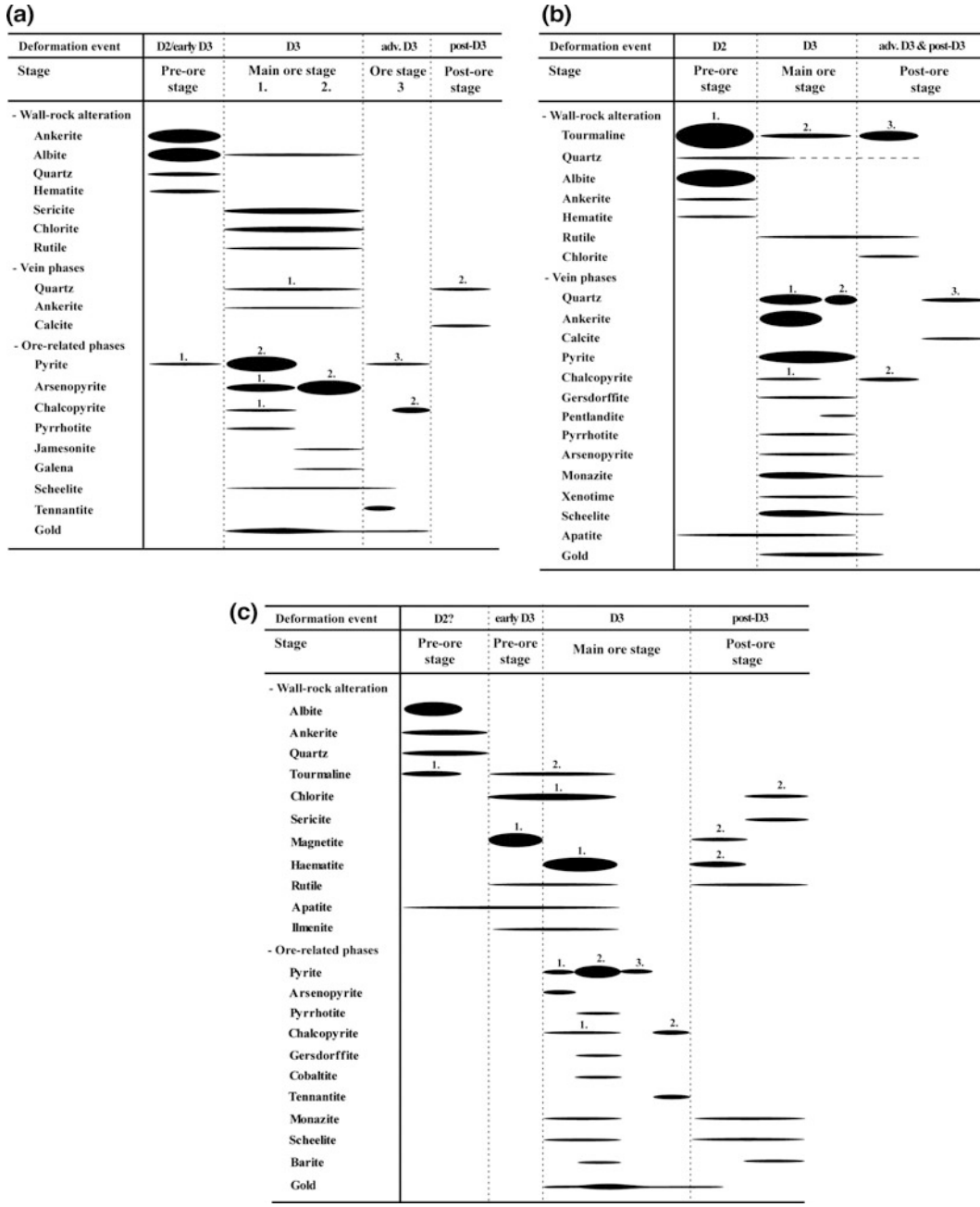

Fig. 4 Paragenesis of veins ore, and alteration zones for Yalea (**a**), Gara (**b**), and Gounkoto (main ore body; **c**). Data from Lawrence et al. (2013a)

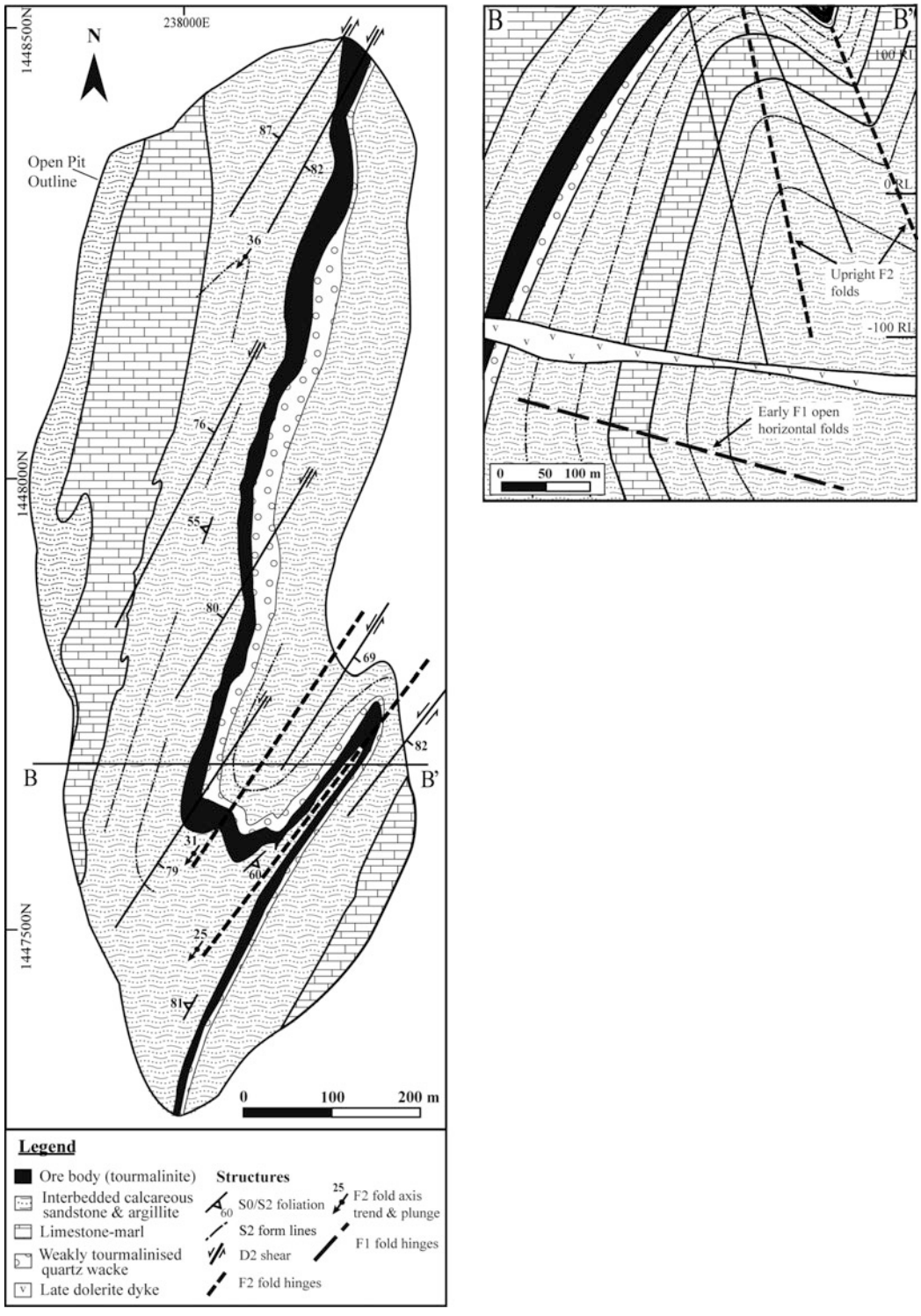

Fig. 5 Geological and structural plan map (*left*) and cross section (*right*) of Gara gold deposit in Loulo district, showing geometry of ore body and multi-phase development of folds

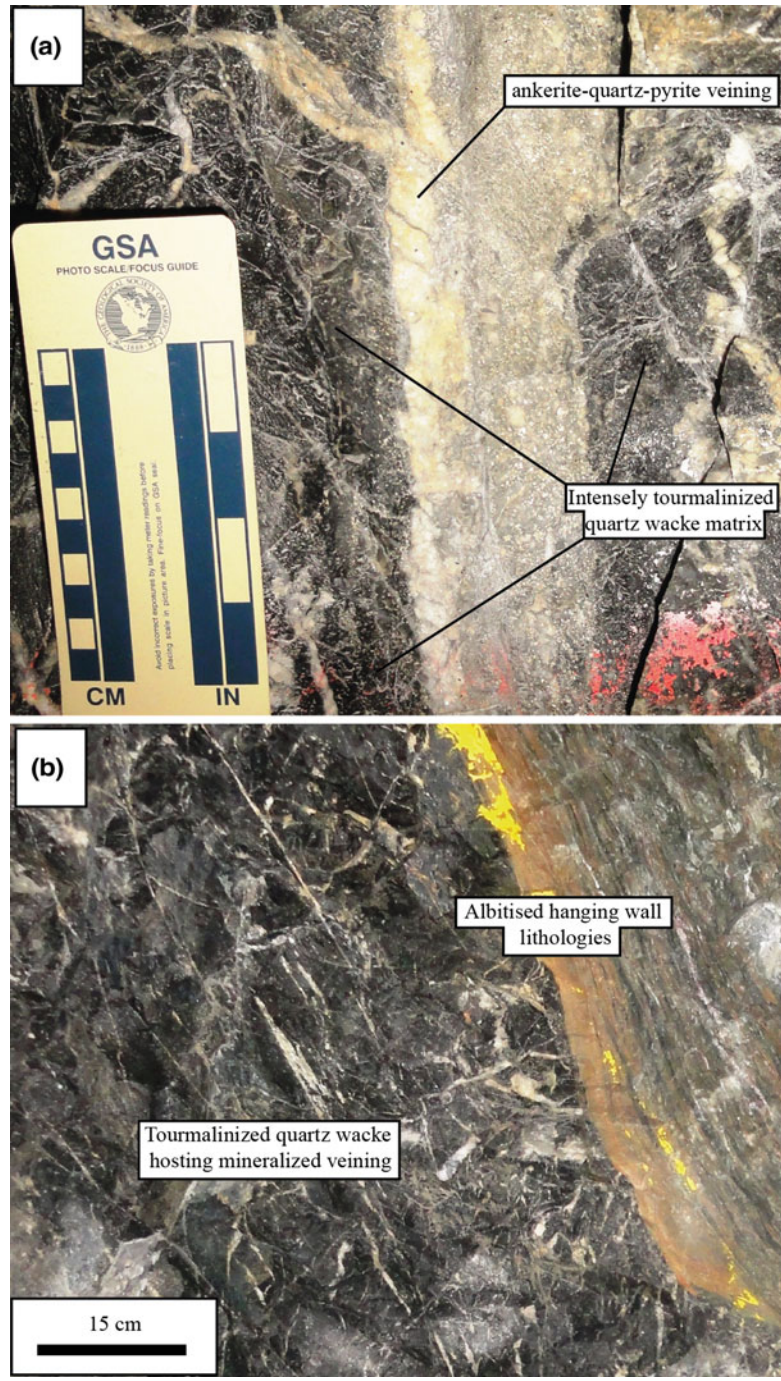

Fig. 6 Photographs of Gara ore showing dark tourmalinite host rocks cut by a stockwork of millimeter- to centimeter-scale quartz-gold-ankerite-pyrite veins

alteration, with an overlapping phase of subordinate tourmaline alteration; (2) magnetite-chlorite ± tourmaline alteration; (3) disseminated sulphide-Au mineralization; (4) replacement by magnetite and Au remobilization; and (5) minor replacement by hematite-sericite-chlorite (Fig. 4c). Ore minerals comprise pyrite and arsenian pyrite (≤ 2 wt% As), accompanied by minor to

trace amounts of chalcopyrite, arsenopyrite, pyrrhotite, tennantite, cobaltite, gersdorffite, scheelite, and monazite. Gold-bearing minerals consist of native gold (fineness > 980) and Au ± Ag tellurides including calaverite ($AuTe_2$), sylvanite (Ag, Au)Te_2, and petzite (Ag_3AuTe_2).

Hanging-wall mineralization at Gounkoto is disseminated within a 20-m-thick dolomitic limestone. These minor ores comprise nickeloan pyrite (max. 13 wt% Ni), Ni-rich cobaltite, clausthalite (PbSe), and chalcopyrite, with lesser galena, sphalerite, and other Ni-bearing sulphides. Gold is texturally associated with all major generations of sulphides.

4.1.4 Fluid Inclusion and Stable Isotope Data

Lawrence et al. (2013b) recently documented the petrography, geothermometry, and chemistry of fluid inclusion assemblages at the Gara and Yalea gold deposits. Four fluid inclusion types are recognized as being coeval with ore formation: (1) $CO_2 \pm N_2 \pm CH_4$ inclusions; (2) low-salinity H_2O–NaCl inclusions (≤ 10 wt% NaCl equiv.); (3) H_2O–CO_2–NaCl $\pm$ N_2 $\pm$ CH_4 inclusions; and (4) multi-phase H_2O–CO_2–NaCl–$FeCl_2$ $\pm$ CH_4 $\pm$ N_2 brines (Fig. 7). Type 4 inclusions contain daughter minerals, including NaCl, $FeCl_2$, Fe_2O_3, Fe_3O_4, and carbonates. All inclusion types are present within the Gara and Gounkoto ore bodies; however, hypersaline fluid inclusions are absent from Yalea.

Stable isotope data (Fouillac et al. 1993; Lawrence et al. 2013b) were used to determine the source of volatile ore-forming components (O, C, and S) at Loulo. Measured $\delta^{18}O_{quartz}$ values are remarkably homogenous (Fig. 8a) both for mineralized samples (+16.3 ± 0.3 ‰; $n = 20$) and barren quartz veins (+15.9 to +17.0 ‰; $n = 4$). Measured $\delta^{18}O_{carbonate}$ values for samples of mineralized veins and wall-rock alteration are more variable (15.9 ± 2.1 ‰; $n = 20$). In contrast, barren calcite veins display $\delta^{18}O$ values of +15.1 to +21.1 ‰ ($n = 5$) (Fig. 8b). Estimated $\delta^{18}O_{fluid}$ compositions for gold-bearing veins at Gara and Yalea range from +9 to +12 ‰. Carbonates associated with mineralization at Loulo show $\delta^{13}C$ values from −21.7 to −4.5 ‰ ($n = 20$) (Fig. 8c); barren calcite veins are isotopically heavier ($\delta^{13}C$ −2.0 to +3.8 ‰; $n = 5$), closely matching the values of the Kofi Series limestones (−2.9 to +1.3 ‰; $n = 6$). Auriferous sulphides display $\delta^{34}S$ values of +5.8 and +15.5 ‰ ($n = 27$) (Fig. 8d). Diagenetic pyrite from wall rock at Yalea has sulphur isotope compositions of +6.4 to +9.0 ‰ ($n = 2$).

4.1.5 Loulo-Gounkoto Ore Genetic Model

Ore bodies within the Loulo-Gounkoto district share many features typical of orogenic gold deposits such as a late-orogenic timing of mineralization, and strong regional and local structural controls on ore formation. Within this framework, Lawrence et al. (2013a, b) detailed two separate end-member styles of orogenic gold mineralization in the region (termed Gara- and Yalea-style) based on different ore and alteration mineralogy, and ore-fluid compositions. The Gara and Gounkoto deposits are characterized by: (1) predominance of pyrite; (2) distinct metal signatures enriched in Fe-REE-W and locally base metals (e.g., Gounkoto hanging-wall mineralization); (3) strong tourmaline alteration atypical of orogenic gold deposits (e.g., Groves et al. 1998); and (4) presence of brines in fluid inclusions. Conversely, Yalea-type deposits (Yalea and satellite ore bodies along the Yalea Trend) have a more typical Birimian orogenic gold ore mineralogy, wall-rock alteration, and ore fluid characteristics (cf. Milési et al. 1992; Allibone et al. 2002a, b; Béziat et al. 2008). These latter ore bodies: (1) are As-rich; (2) lack a REE-base metal enrichment; (3) have alteration assemblages dominated by quartz-carbonate-albite and sericite-chlorite (tourmaline-absent); and (4) lack brines in fluid inclusions.

Lawrence et al. (2013b) interpreted the various fluid inclusion assemblages as representing two distinct end-member fluids: (1) a high-temperature, high-salinity, CO_2-poor, aqueous fluid (~400 °C; ~45–55 wt% NaCl equiv.; X_{H2O} of 0.7–0.8; $X_{CO2} < 0.3$); and (2) a lower temperature, more dilute, aqueous-carbonic fluid (270–350 °C; <10 wt% NaCl equiv.). Partial mixing between these fluids

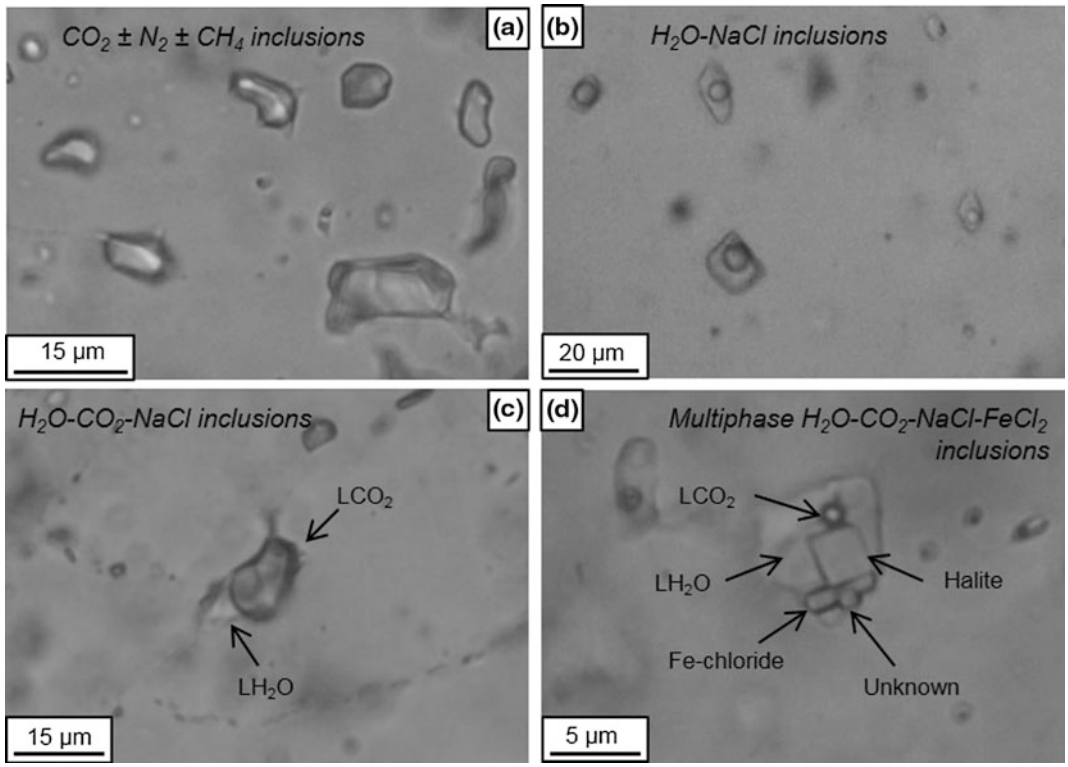

Fig. 7 Photomicrographs (taken at room temperature) of fluid inclusion types present in mineralized samples from Loulo district. **a** Single phase $CO_2 \pm N_2 \pm CH_4$ inclusions, **b** two-phase H_2O–NaCl inclusions, **c** rare H_2O–CO_2–NaCl inclusions, and **d** multi-phase, hyper-saline, H_2O–CO_2 inclusions with halite and Fe-chloride daughter minerals. *L* liquid phase; *V* vapor phase

during formation of the Gara-style ore bodies resulted in retrograde boiling ("salting out effect"; e.g., Anderson et al. 1992) and changes in the physicochemical state of both fluids, leading to precipitation of sulphide minerals and Au. At Yalea, the hypersaline fluid is absent and fluid inclusions contain two immiscible phases derived from the phase separation of a dilute, aqueous-carbonic fluid. Fluid immiscibility likely occurred in response to pressure-temperature fluctuations along the Yalea Shear and/or fluid-rock interaction with the hanging-wall carbonaceous limestone cap. The combination of microthermometric data and geothermometry based on ore and alteration assemblages indicates that mineralization occurred at mesozonal temperatures and pressures of 270–340 °C at 1.4–1.8 kbar (5.5–6 km) (Lawrence et al. 2013b).

The presence of a dilute aqueous-carbonic hydrothermal fluid is consistent with a metamorphic source for this fluid (e.g., Phillips and Powell 2010). Supporting evidence comes from stable isotope (O, C, and S) data that suggest devolatilization of a sedimentary sequence. Oxygen isotope values show $\delta^{18}O_{fluid}$ compositions between +9 to +12 ‰ that are similar to those of metamorphic fluids (cf. Ohmoto and Goldhaber 1997). Carbon isotope data for auriferous veins and hydrothermal alteration at Loulo fall on a tie line between ^{13}C-depleted organic carbon (−24.7 ± 6 ‰; Schidlowski et al. 1983) and inorganic carbonate minerals occurring in the host limestone (−2.9 to +1.3 ‰). On this basis, CO_2 is likely to have been sourced directly by the dissolution of carbonate-rich units in the host terrane during pro-grade metamorphism, and indirectly by fluid-rock interactions at the site of

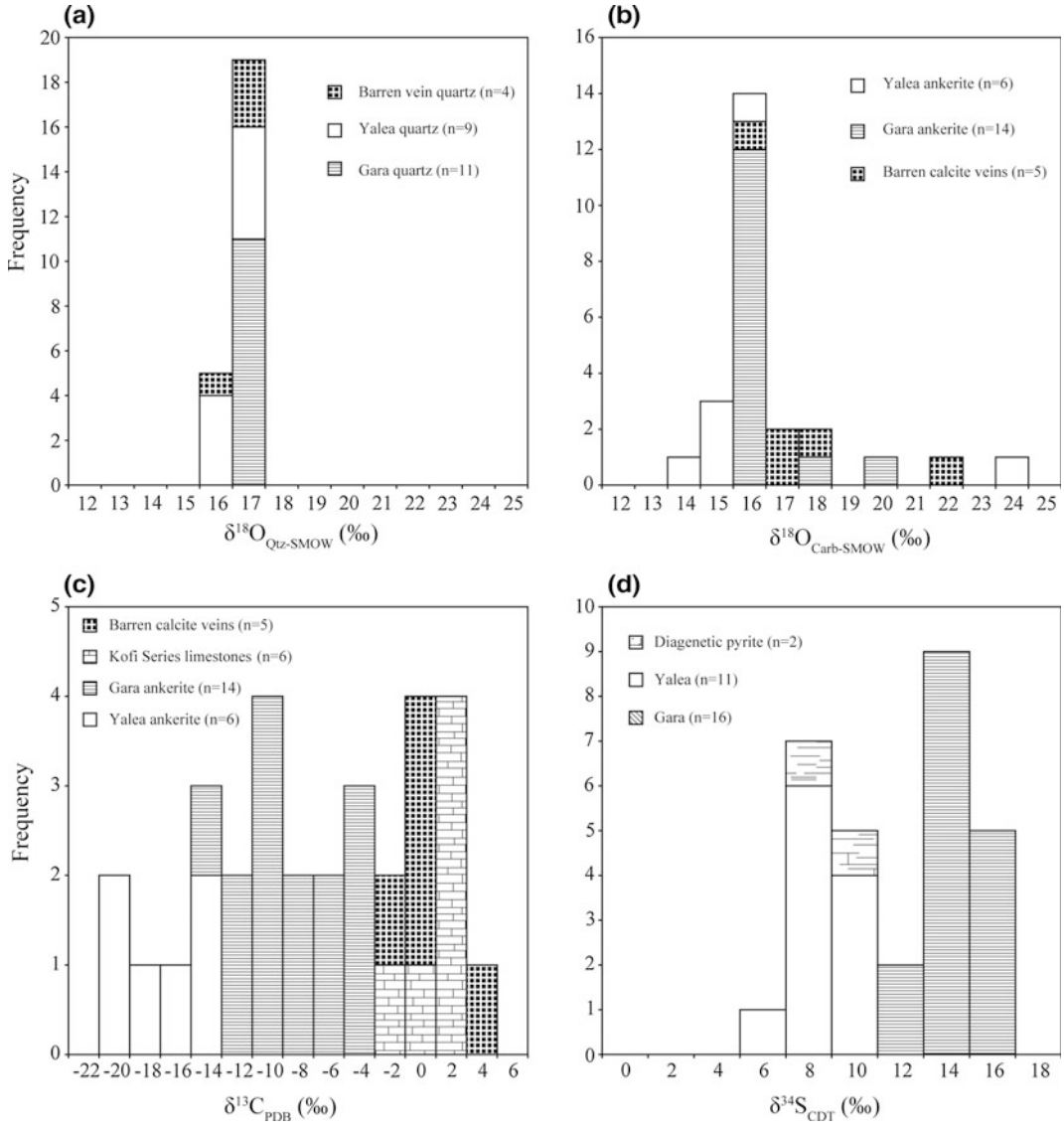

Fig. 8 Histograms showing $\delta^{18}O_{silicate}$, $\delta^{18}O_{carbonate}$, $\delta^{13}C_{carbonate}$, and $\delta^{34}S_{sulphide}$ stable isotope data for mineralized and non-mineralized rocks at Yalea and Gara (data compiled from Fouillac et al. 1993; Lawrence et al. 2013b; Lambert-Smith 2014)

ore formation. The $\delta^{34}S$ values of the ore sulphides (+5.8 to +15.5 ‰) broadly match limited $\delta^{34}S$ data for diagenetic pyrite in the Kofi Series (+6.4 to +9.0 ‰); this pattern suggests that sulphur was derived by the devolatilization of diagenetic pyrite in the host sedimentary terrane (cf. Tomkins 2010; Large et al. 2011; Gaboury 2013).

The hypersaline, aqueous-rich fluid inclusions present in the Gara-style deposits, together with the metal associations and intense tourmaline alteration, suggest that a magmatic fluid contributed to the Loulo ore-forming system (Lawrence et al. 2013a, b). However, the lack of a magmatic signature in the stable isotope dataset allows for a possible alternative fluid

origin in which brines were sourced from B-rich evaporite units within the Kofi Series. In this model, mixing of hypersaline fluids with regional, low-salinity, aqueous-carbonic metamorphic fluids led to the formation of atypical (Gara-style), tourmaline-rich, orogenic gold deposits in the Loulo district.

4.2 Sadiola

The Sadiola deposit is 120 km north of the Loulo-Gounkoto complex, in the northern part of the Kédougou-Kéniéba inlier (KKI) (Fig. 1c). The mine was officially opened in 1996 (and together with Yatela) is owned by Société des Mines d'Or du Mali (SEMOS), a joint venture between AngloGold Ashanti Limited, IAMGOLD Corporation, and the Malian government. Current probable reserves at Sadiola are 3.8 Moz of Au at an average grade of 2.1 g/t (IAMGOLD Corporation 2014).

4.2.1 Deposit Geology and Structure

The Kofi stratigraphy at Sadiola consists of a thick (>250 m) limestone-marl sequence that strikes N-S to NNW and dips 60–65° to the west, and is overlain by a hanging-wall unit composed of sandstone with interbedded siltstone and mudstone (Figs. 9 and 10). The contact between the two lithologic domains is structurally controlled by the mineralized brittle-ductile Sadiola Fracture Zone (SFZ), a splay off the Senegal-Mali Shear Zone (SMS). The SFZ is 10–50 m wide and consists of an anastomosing network of fractures and shears. Sedimentary rocks exposed in the Sadiola Hill open pit are cut by three successive generations of intrusions (Fig. 9), which include: (1) early diorite stocks, discontinuous dikes and sills, which were emplaced parallel to sub-parallel to bedding at the contact between carbonate and siliciclastic units; (2) sub-vertical, narrow (<5 m), NNE-trending, quartz-feldspar-phyric granodiorite dikes; and (3) a series of 1–2-m-wide, ENE-trending, dolerite dikes that cut the granodiorite dikes.

The Sadiola structural model proposed by Masurel et al. (in press) is similar to that outlined previously for the Loulo-Gounkoto district. Three main deformation events have been recorded. The first phase of deformation (D1) is associated with NNW-trending recumbent folding (F1) and the development of sub-horizontal, hinge-parallel, lineation. This event remains poorly constrained owing to poor exposure and reworking during later deformation. D2 deformation is linked to upright to inclined F2 folds that plunge gently (15–30°) to the SSW and have an axial-planar cleavage of 020°/75° E. NNE-trending thrusts, high-angle reverse faults, and quartz-feldspar-phyric dikes are spatially closely associated with these F2 folds. The N-S-trending SFZ is interpreted to have been initiated as a sinistral reverse fault during the latter part of D2.

D3 marks a switch from predominantly pure shear (folding and reverse faulting with minor strike-slip displacement during D2) to a simple-shear system. Fault geometries and kinematic indicators are consistent with NNW-SSE-directed shortening. Evidence for sinistral strike-slip movement is present in wall-rock limestones in close proximity to the SFZ, with steeply plunging parasitic folds showing pronounced S-shaped asymmetry. Mapping in the open pit has identified the occurrence of drag folds within the main structure, correlating with F2 folds and re-oriented along a N-S axis. Minor post-D3 brittle deformation is also present including late extensional quartz veins <30 cm wide and sub-vertical brittle faults 10 cm to >10 m in width (Fig. 9).

Structural data suggest that gold mineralization is confined to a single deformation event (D3) (Masurel et al. in press). The bulk of the ore is hosted within the SFZ and the deformed limestones in the adjacent footwall. Ore also occurs along the reactivated NNE-trending faults, although grades decrease with increasing distance from the SFZ. Mineralization is mainly present as zones of disseminated sulphides; minor sulphide veinlets and quartz-carbonate-sulphide ± biotite-tourmaline veins occur locally. A range of ductile to brittle ore textures are observed. Ductile shearing within the SFZ is commonly associated with gold grades of >10 g/t. Ductile textures are best observed in diorite dikes where fine-grained sulphides are consistently

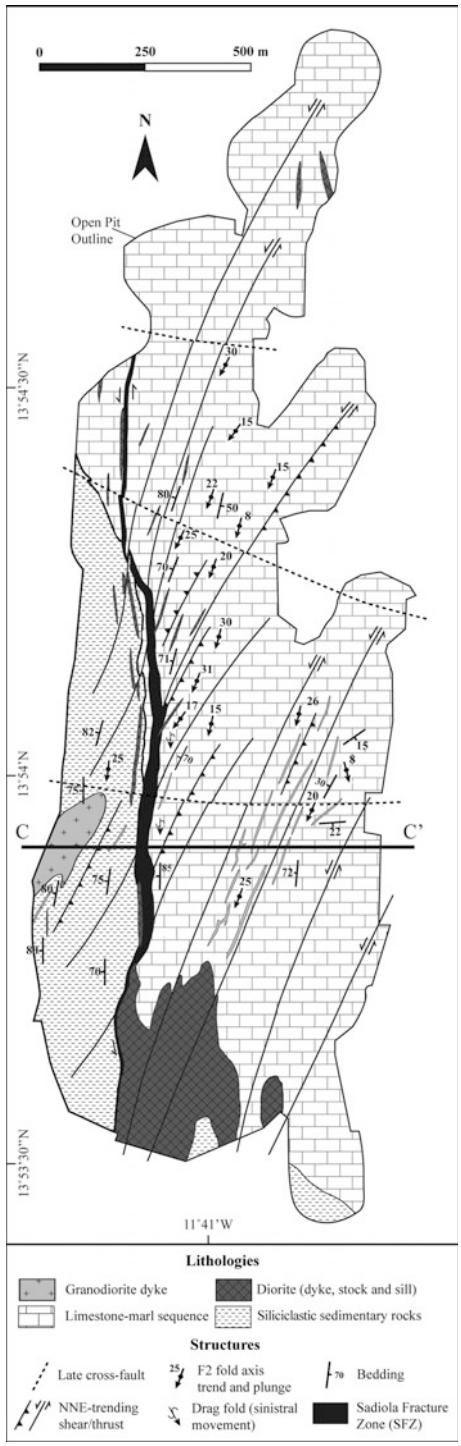

Fig. 9 Geological and structural map of Sadiola open pit (modified from Masurel et al. in press). Gold mineralization is largely confined to the Sadiola Fracture Zone. Cross section C–C′ is shown in Fig. 10

aligned parallel to the shear fabric. Brittle textures are well developed in the footwall limestones, characterized by randomly oriented dolomite stockworks and crackle breccias commonly sealed by sulphides. These hydrothermal-tectonic breccias form wide zones of low to medium grade mineralization (ca. 1 to 3 g/t Au).

4.2.2 Alteration and Mineralization

Masurel et al. (in press) reported a polyphase hydrothermal alteration history for the Sadiola deposit that involves an early calc-silicate phase followed by a potassic alteration stage (Fig. 11). The early high-temperature alteration is confined mainly to Ca-rich host rocks (limestone and mafic-intermediate dikes) and is represented by porphyroblastic actinolite and tremolite. This style of alteration is strongly developed within the SFZ and to a lesser extent along the NNE-trending faults. The calc-silicate alteration phase is overprinted by a later, syn-mineralization, potassic alteration stage, which contains a mineral assemblage dominated by biotite-(phlogopite), calcite-dolomite, and quartz, plus minor tourmaline (dravite), sericite, and microcline. The last stage of hydrothermal alteration recognized at Sadiola is associated with D5 normal reactivation of ore-hosting structures and the formation of numerous chlorite-calcite pyrite veins.

Ore sulphides related to the potassic alteration stage commonly form concentrations of 0.5 to 3 vol%. Paragenetic studies indicate a multi-stage ore development consisting of an early arsenopyrite-rich Au phase (Stage 1), and later Sb ± Au phases (Stages 2–3) (Fig. 11). Stage 2 comprises pyrrhotite + berthierite ($FeSb_2S_4$) + stibnite + native gold + aurostibite, whereas Stage 3 is characterized by native Sb + native Bi + Sb–Ni–Pb sulphosalts (e.g., gudmundite, ullmannite, jamesonite).

4.2.3 Sadiola Ore Genetic Model

Orogenic gold mineralization at Sadiola shows similar regional and local structural controls to that observed along the southern part of the Senegal-Mali Shear Zone (SMS). However in contrast to Loulo, ore and wall-rock alteration assemblages at Sadiola show distinctive features

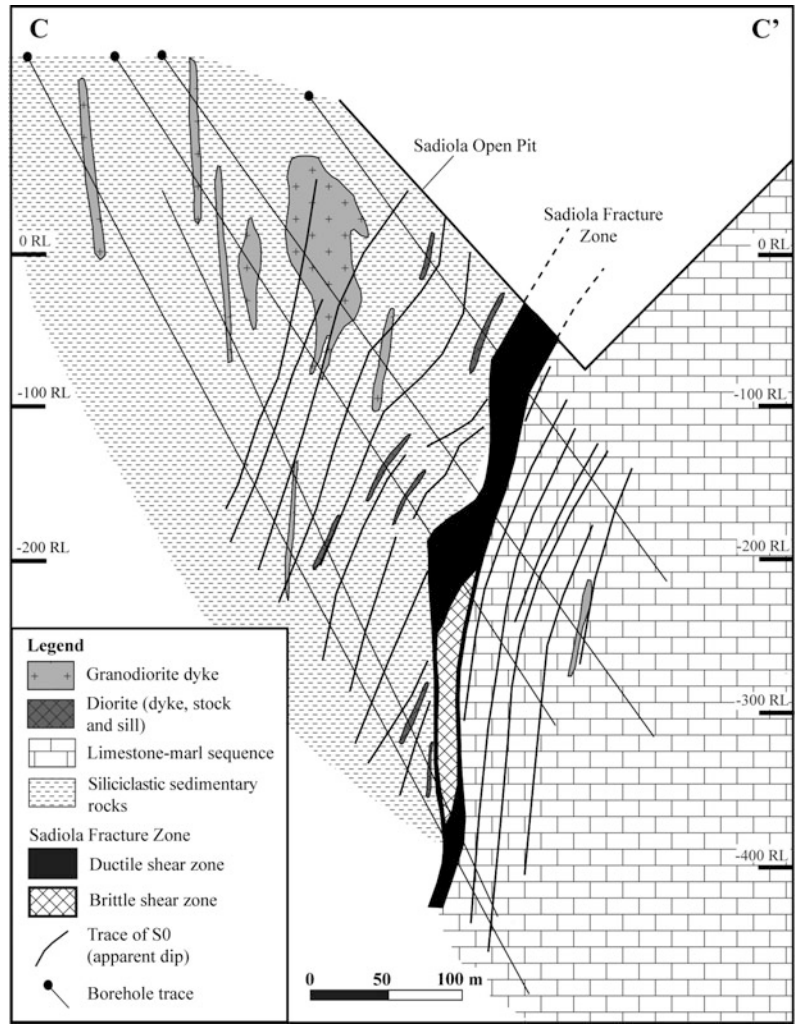

Fig. 10 Cross section through southern part of Sadiola ore body (cross section C–C′ on Fig. 9) showing geometry of Sadiola Fracture Zone (modified from Masurel et al. in press)

such as early high-temperature calc-silicate alteration, and later Au–Sb–Te–Bi mineralization typical of low temperature, epizonal (<6 km) orogenic gold deposits (cf. Groves et al. 1998). Combined field, mineralogical, geothermometric, and micro-textural data suggest that the multi-phase ore and alteration development at Sadiola reflects a hydrothermal cooling continuum in the temperature range of 400 to 260 °C, rather than representing contrasting mineralization styles at distinct crustal levels (Masurel et al. in press). Although rare, calc-silicate alteration has been reported in some amphibolite-hosted Precambrian orogenic gold deposits (McCuaig et al. 1993; Smith 1996), where the temperature of the mineralizing fluid was high enough to stabilize calc-silicate minerals in Ca-rich host rocks (McCuaig and Kerrich 1998). In contrast, the early ore and alteration paragenesis at Sadiola is in thermal disequilibrium with the greenschist-facies metamorphosed host rocks, hence the thermal gradient likely reflects the input of D3 Eburnean magmatism and related hydrothermal circulation in the region (Masurel et al. in press).

The Massawa orogenic gold deposit, located along the western (Senegalese) side of the Kédougou-Kéniéba inlier 80 km to the southwest of Sadiola, shares a similar deposit paragenesis albeit with the absence of calc-silicate alteration.

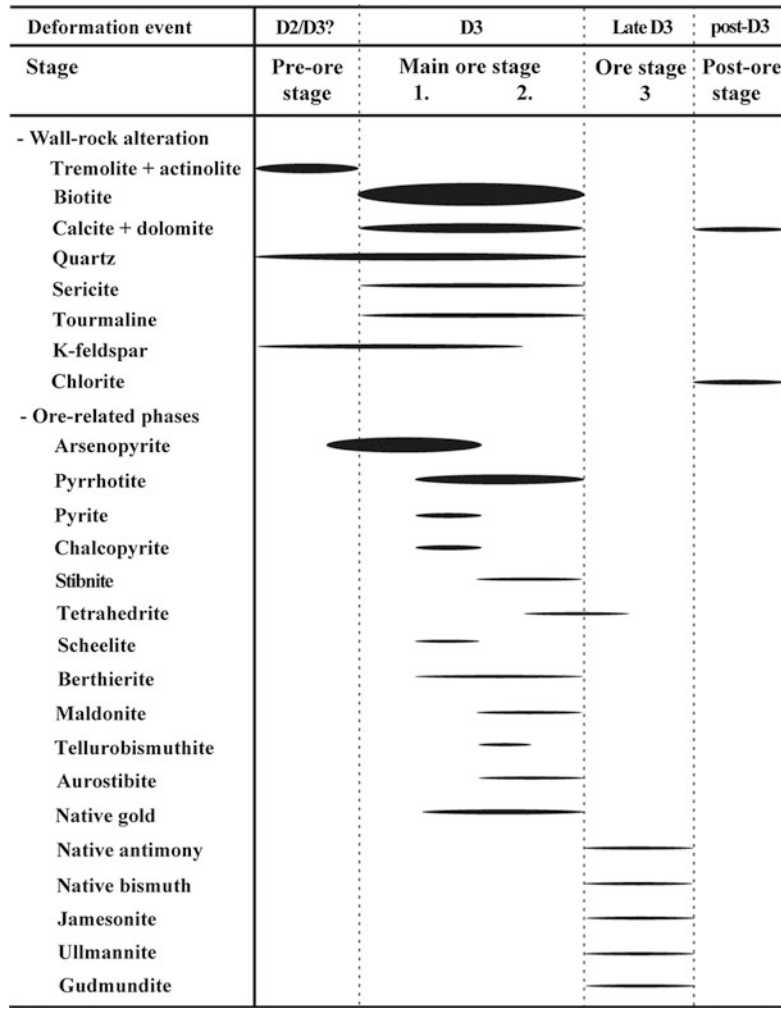

Fig. 11 Paragenesis of ore and alteration zones for the Sadiola deposit (modified from Masurel et al. in press)

The Massawa deposit is characterized by predominantly brittle deformation, widespread potassic alteration (mainly sericite) synchronous with disseminated arsenopyrite-pyrite mineralization, and a second phase of high-grade quartz-stibnite veins with coarse visible gold (Treloar et al. 2014a). Combined field relationships, fluid inclusion data, and stable isotope values suggest a magmatic fluid influence on gold mineralization in Massawa deposit, with ore formation occurring at epizonal depths (4–6 km) with a temperature-pressure range of 220–315 °C at 1–1.65 kbar (Treloar et al. 2014a).

4.3 Yatela

The Yatela gold mine is 25 km north of Sadiola, 50 km SSW of the regional capital of Kayes. Production began in 2001 by Société des Mines d'Or du Mali (SEMOS). The deposit geology comprises a Kofi limestone-marl package intruded by a dioritic pluton, both units being overlain by Upper Proterozoic Seroukoto sandstone of the Taoudeni basin. Primary gold mineralization is hosted in shear zones and localized along the lithologic contact between the limestone and diorite; spatially associated is disseminated pyrite

and an alteration assemblage of albite, sericite, and dolomite. Significantly, economic gold mineralization is supergene in origin and linked to karstic dissolution of the Kofi limestone (Hanssen et al. 2004). The weathering profile is characterized by deep troughs (maximum of 220 m) above the limestone, with infill sequences consisting of a basal unit composed of unconsolidated ferruginous, sandy, and locally clayey material, overlain by pisolithic gravels, laterite rubble, and fine-grained sands. The basal ferruginous layer represents the gold-enriched dissolution residue of the mineralized carbonate protolith (Hanssen et al. 2004).

5 Reduced Intrusion-Related Gold Systems

5.1 Morila

The multi-million ounce, world-class, Morila gold deposit is in southern Mali, 180 km south of Bamako and close to the town of Sanso (Fig. 1b). The mine has produced more than 7 Moz of gold at ~4.6 g/t since commissioning in 2000, and is predicted to produce a further estimated 267 Koz at 0.66 g/t from open pit extensions and stockpiles over the next few years (Randgold Resources Ltd 2014). Early exploration carried out by BUGECO in 1987 identified several large gold anomalies in soils. In 1992, BHP Minerals Mali acquired the rights to the area and carried out initial exploration drilling. Although this work returned encouraging results, BHP ceased exploration in Mali in 1996. Randgold Resources acquired BHP Minerals Mali and commenced detailed exploration of the Morila permit, which led to the discovery of the Morila deposit. In 2000, AngloGold Ashanti purchased 40 % of Morila with Randgold Resources retaining 40 % and the Government of Mali 20 %.

5.2 Deposit Geology and Structure

The Morila deposit is located within the Bougouni terrane that is characterized by a volcano-sedimentary sequence intruded by large granitoid batholiths and numerous smaller mafic to felsic bodies (Liégeois et al. 1991) (Fig. 1b). Deposit geology is characterized by a NW-trending package of turbiditic metasedimentary rocks bounded to the east and northeast by the Massigui Granite and to the southwest by the Doubalaokoro tonalite-trondjhemite-granite (TTG) suite (Fig. 12). The metasedimentary rocks comprise a 1-km-thick monotonous sequence of medium- to coarse-grained, moderately to poorly sorted, biotite-rich, feldspathic wacke. Subtle lithologic variations occur locally with interbeds composed of finer-grained meta-pelitic rocks and meta-basalts. Within the siliciclastic rocks, beds have sharp bases, grade upwards, and show pronounced soft-sediment deformation features typical of turbidite systems such as flame structures and load clasts (McFarlane et al. 2011). Sedimentary rocks in the vicinity of Morila have contact metamorphic assemblages typical of amphibolite-facies conditions, including abundant hornblende in the meta-basalts and cordierite and andalusite preserved in the more pelitic rocks.

Several intrusions are emplaced into the meta-sedimentary sequence of the Morila permit area (McFarlane et al. 2011). The oldest of these are thin (5–10 m), porphyritic mafic to intermediate-composition hypabyssal dikes for which geochemical data suggest a continental margin setting. These rocks are pre-orogenic and have U–Pb zircon ages of 2132 ± 4 to 2131 ± 5 Ma. Younger and more felsic, sub-alkaline, D2 intrusive bodies are represented by the Morila Tonalite (including quartz diorite) and the Doubalakorou suite of fine- to medium-grained biotite-rich granodiorite and coarser, foliated monzogranite; these intrusions yield U-Pb zircon crystallization ages of 2098 ± 4 to 2091 ± 4 Ma, respectively. Hornblende and cordierite-andalusite hornfels are concentrated around these D2 intrusive rocks. The Morila tonalite and Doubalakorou felsic rocks are post-dated (2075 ± 12 Ma; Armstrong 2003) by the Massigui leucogranite (post-D2 origin; D3?).

The Morila gold deposit is a flat-lying tabular body that dips gently to the east (0–30°) and

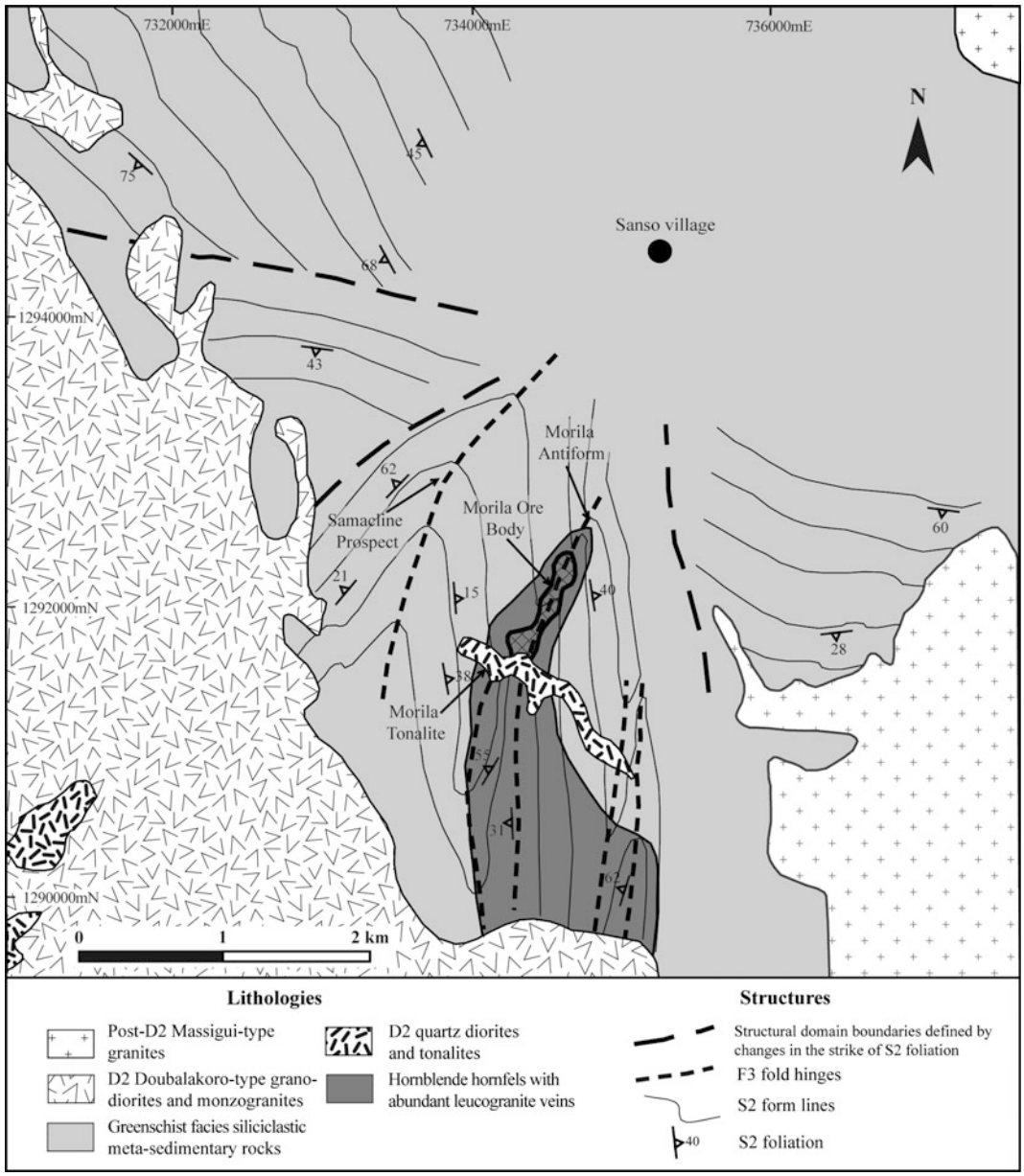

Fig. 12 Geological and structural map of Morila district. Main deposit and nearby Samacline prospect to northwest are located in hinge zones of upright F3 folds within domains of gently dipping S2 foliation. Hornblende-hornfels contact metamorphism is present in vicinity of Morila ore body, which extends southward towards Doubalakoro pluton (modified from King 2012)

varies in thickness from 25–160 m, with thicknesses increasing to the south and west close to contact with the Morila Tonalite (Fig. 13). A sub-parallel lode (Samocline prospect) is intersected at depth below the main deposit. The main ore body is truncated on its northern side by a steep fault (exposed on the northern wall of the Morila open pit) that is downthrown to the north. Displacement along this fault is likely to be significant because metasedimentary rocks to the

north show lower (greenschist facies) metamorphic grades and deep drilling has failed to intersect significant mineralization north of the fault. McFarlane et al. (2011) identified two stages of folding associated with D2 and post-D2 deformation: (1) recumbent F2 isoclinal folds that developed in a fold and thrust belt, accompanied by a strong S2 schistosity; and (2) more widespread, upright, open F3 N- to NNE-trending folds (Fig. 13). High-grade gold mineralization at Morila (avg grade > 10 g/t) is concentrated along the fold hinge of an F3 fold, known locally as the Morila antiform.

5.3 Alteration and Mineralization

King (2012) reported two main phases of hydrothermal alteration and associated gold mineralization at Morila. This interpretation is generally consistent with the results of both McFarlane et al. (2011) and Hammond et al. (2011), and builds on data presented by Quick (1999) (Fig. 14). Pervasive biotitization is synchronous with the penetrative S2 schistosity, and is spatially associated with millimeter- to centimetre-scale polymetallic (Au–Sb–Bi–Te) quartz veins having varying concentrations of hornblende, biotite, plagioclase, and fluorapatite. Sulphide assemblages consist of löllingite, pyrrhotite, and chalcopyrite. Free native gold (avg 940 fineness) is associated with scheelite, native bismuth, maldonite (Au_2Bi), aurostibite ($AuSb_2$), and tellurobismuthite (Bi_2Te_3). Au–Sb–Bi–Te mineralization is spatially and temporally associated with metasomatic zones that surround D2 granodiorite and quartz diorite intrusive stocks and associated dikes.

Following stage 1 mineralization, the Morila host rocks were pervasively albitized and sulphidized during post-D2 mineralization. This phase of gold mineralization is largely confined to the NE-trending fold hinge of the F3 Morila antiform, where gold was remobilized into high-grade ore shoots. Coarse-grained idioblastic arsenopyrite, which cuts earlier deformation

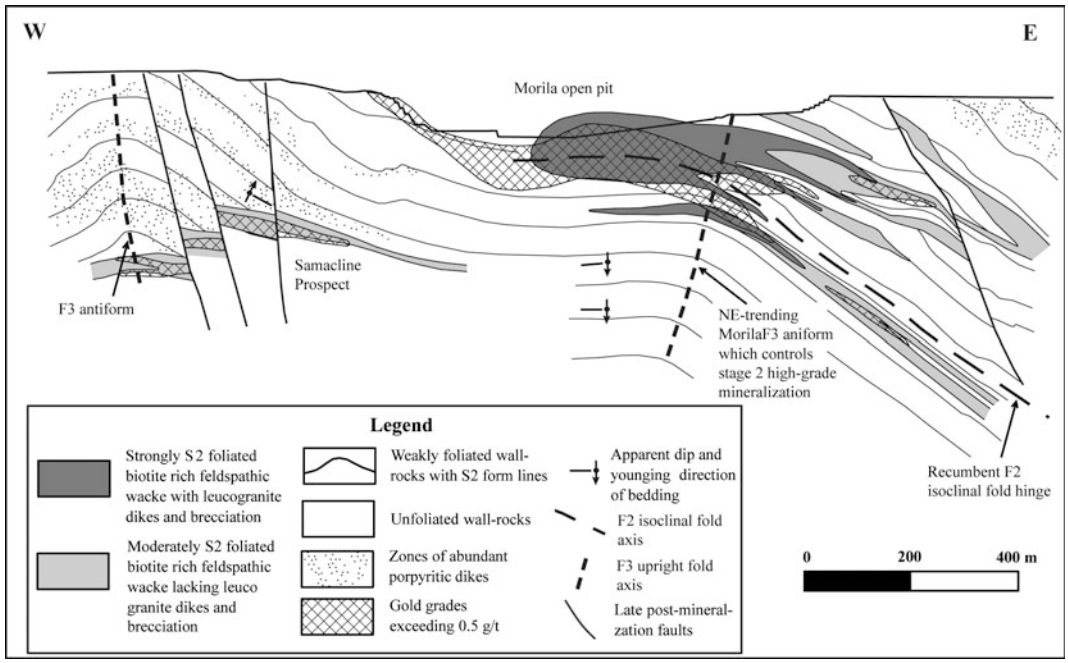

Fig. 13 Typical E-W cross section through the Morila deposit showing geometry of the ore body and multi-phase folds (modified from McFarlane et al. 2011)

fabrics, contains partially resorbed cores of löllingite with blebs of native gold (5–25 μm; fineness of 850) located along mineral boundaries. McFarlane et al. (2011) dated titanite associated with arsenopyrite that yielded a preliminary age for late-stage sulphidation of 2074 ± 14 Ma, which brackets mineralization as a whole to the interval 2098 ± 4 to 2074 ± 14 Ma. McFarlane et al. (2011) also identified a minor late vein stage containing chlorite-pyrite-quartz or quartz-plagioclase-apatite-tourmaline ± molybdenite ± beryl, accompanied by alteration selvages of cordierite, biotite, chlorite, and plagioclase.

5.4 Fluid Inclusion and Stable Isotope Data

Fluid inclusion and stable isotope investigations at Morila have been carried out by Quick (1999) and Hammond et al. (2011). Both studies identified similar fluid inclusion assemblages for both phases of mineralization. Two end-member fluids are distinguished, one a H_2O–NaCl ± N_2 ± CH_4 fluid characterized by high-temperatures (250–400 °C) and low to moderate salinities (0.5–8.0 wt % NaCl equivalent), and another a $CaCl_2$-bearing brine with low temperatures (100–200 °C) and higher salinities (20–32 wt% NaCl equivalent).

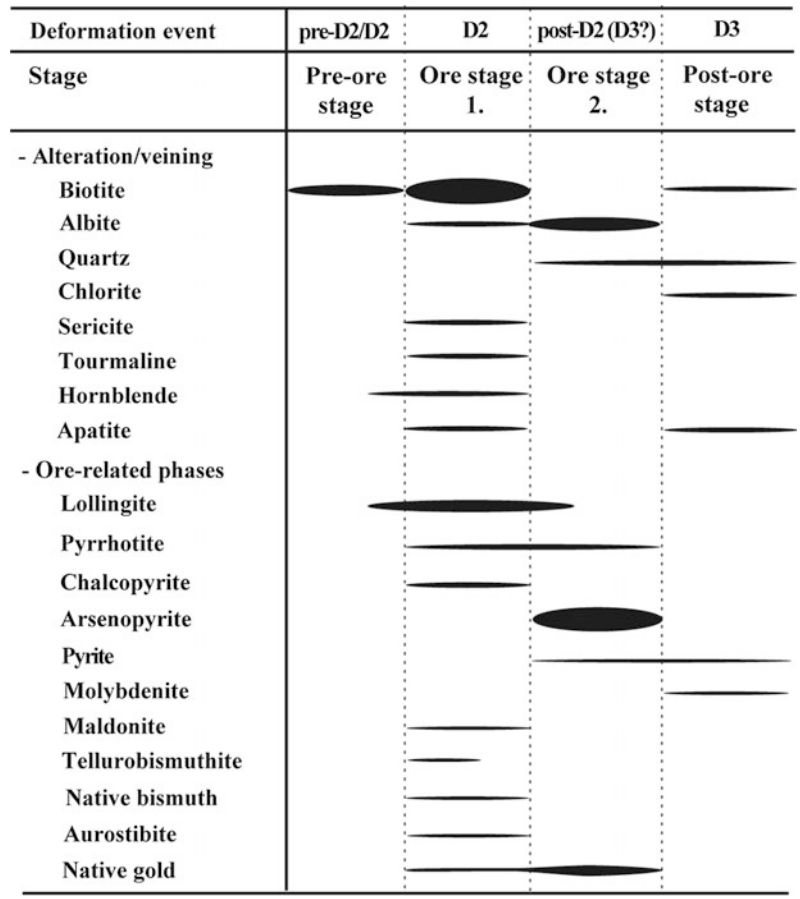

Fig. 14 Paragenesis of ore and alteration zones for the Morila deposit (data from McFarlane et al. 2011; King 2012)

Oxygen isotope data reported by Hammond et al. (2011) from quartz-biotite pairs indicate average $\delta^{18}O_{fluid}$ values of 9.8 ± 0.3 ‰ and 10.9 ± 0.3 ‰ for fluids that flowed through unmineralized and mineralized host rocks, respectively. Sulphur isotope data of Quick (1999) and Treloar et al. (2014b) show a unimodal distribution of $\delta^{34}S$ values between 2 and 5 ‰ for auriferous arsenopyrite from stage 2 mineralization.

5.5 Morila Ore Genetic Model

Morila is characterized by several features that are inconsistent with a conventional orogenic gold classification for the Birimian deposits. These include: (1) the sub-horizontal strata-bound ore geometry, which contrasts with the steeply dipping, tabular morphology typical of shear-hosted orogenic gold deposits (cf. Groves et al. 1998; Ridley and Diamond 2000); (2) the syn-metamorphic timing of gold mineralization (orogenic gold mineralization generally forms during post-peak metamorphism; Groves et al. 2000); and (3) the moderate salinity of the ore fluids, which is distinctly different from the low salinities (<10 wt% NaCl equiv.) and CO_2-rich nature of fluids that formed many Birimian gold deposits (excluding Gara) (e.g., Klemd et al. 1996; Schmidt Mumm et al. 1997).

The strata-bound geometry of the ore body appears to be lithologically controlled. Hammond et al. (2011) and McFarlane et al. (2011) reported higher Mg/(Mg + Fe) ratios in biotite and an increase in chalcophile elements (Cu, Ni, and Zn) in mineralized rocks compared to the immediate footwall and hanging-wall rocks, as well significantly elevated Cr contents in the ore zone from background levels of ~175 ppm to >300 ppm. Hammond et al. (2011) also noted decreases in the anorthite content of plagioclase from wall rocks to the mineralized zone ($An_{51–53}$ to An_{40}, respectively). McFarlane et al. (2011) postulated that mineralization is confined to deformed basaltic volcanic rocks. Although this model is inconsistent with the entire data set, the chemistry is in agreement with tuffaceous fallout from distal basaltic volcanic eruptions, which would have influenced the trace element chemistry of the host feldspathic wackes. Mafic tuffs will hydrate to smectite that is rheologically weak and thus will be more prone to slip during regional deformation, compared to lithologically different rocks above and below. In our interpretation, access to mineralizing fluids was thus preferentially concentrated along these rheologically weak, smectite-rich zones.

According to this model, stage 1 mineralization must have been initiated prior to contact metamorphism. This scenario is consistent with oxygen isotope geothermometry from Hammond et al. (2011), which shows an overlap in temperature estimates between unmineralized and mineralized rocks. The relative timing of metamorphism and stage 2 arsenopyrite mineralization remains enigmatic, however. McFarlane et al. (2011) dated late sulphidation at 2074 ± 14 Ma (U–Pb SHRIMP dating of tittanite), synchronous with emplacement of the post-D2 Massigui plutonic suite, with gold being remobilized into NE-plunging ore shoots as the tabular ore body was re-folded by F3 folds. If metamorphism predated stage 2 mineralization, as suggested by McFarlane et al. (2011), then equilibrium textures within the hornfelsic rocks necessarily would have been deformed during post-D2 folding in order to open grain boundary fractures to permit sufficient fluid access for gold dissolution and remobilization. In summary, the Morila model consists of Au–Sb–Bi–(W–Te) stage 1 mineralization, focussed by shearing along smectite-enhanced bedding surfaces, which produced the main tabular ore body. This mineralization was followed shortly by D2 hornfelsing and then development of stage 2 As–Au mineralization during post-D2 folding.

Fluid inclusion and isotopic compositions from both phases of mineralization suggest that the observed fluid inclusion assemblages formed by phase separation of a $NaCl–CaCl_2–H_2O–N_2–CH_4$ ore fluid of intermediate salinity (12–16 wt% NaCl equiv.). Oxygen isotope geothermometry from co-existing quartz-biotite pairs indicates a deep-seated fluid source with mineralization temperatures of 400–450 °C (Hammond et al. 2011).

Despite similar $\delta^{18}O_{fluid}$ ranges to that reported at Loulo (Lawrence et al. 2013a), Hammond et al. (2011) proposed a magmatic fluid source for gold mineralization at Morila. This interpretation is consistent with the ore genetic model established by McFarlane et al. (2011), which involves a reduced intrusion-related gold system (RIRGS) of gold mineralization at Morila. Using criteria set out by Hart (2007), Morila shows typical RIRGS characteristics, such as: (1) temporal and genetic association with reduced intrusive stocks and dikes that share geochemical and isotopic characteristics of magmatic processes suggested to enhance metal fertility in RIRGS (Sillitoe and Thompson 1998; Lang and Baker 2001); (2) deposition of native gold and rare tellurobisthmuthite in contact metasomatic zones; (3) the metal association of Au–As–Sb–Bi–(W–Te); and (4) hydrothermal alteration that includes albitization and K-metasomatism.

6 Conclusions

Gold deposits within the West Mali gold belt show many features typical of orogenic gold mineralization, such as geological setting, late-orogenic timing, structural paragenesis, and deposit geometry (cf. Groves et al. 1998; Ridley and Diamond 2000). However, ore fluid compositions, as well as mineralization and alteration assemblages, are highly variable along the belt and distinct sub-classes of orogenic gold mineralization are present (Lawrence et al. 2013a). Recent studies (Lawrence et al. 2013b; Lambert-Smith 2014; Masurel et al. in press) have shown that this variability is caused by multiple fluid sources within the Kofi Series (magmatic fluids, evaporite brines, and regional metamorphic fluids). Supergene enrichment of the orogenic gold lodes is economically important in the northern parts of the Gold Belt, involving karstification of mineralized limestones (Hanssen et al. 2004).

Recent studies at the Morila gold deposit, in the Mali South Goldfields, imply a more diverse Birimian gold metallogenesis. McFarlane et al. (2011) classified Morila as a reduced intrusion-related gold system, in which strata-bound gold mineralization formed early in the Eburnean orogenic cycle (syn-metamorphic) with spatial and genetic links to quartz-diorite, granodiorite, leucogranite, and apophyses of the D2 Doubalakoro pluton.

References

Allibone A, Teasdale J, Cameron G, Etheridge M, Uttley P, Soboh A, Appiah-Kubi J, Adanu A, Arthur R, Mamphey J, Odoom B, Zuta J, Tsikata A, Pataye F, Famiyeh S (2002a) Timing and structural controls on gold mineralization at the Bogoso gold mine, Ghana, West Africa. Econ Geol 97:949–969

Allibone A, McCuaig TC, Harris D, Etheridge M, Munroe S, Byrne D, Ammanor J, Gyapong W (2002b) Structural controls on gold mineralization at the Ashanti deposit, Obuasi, Ghana. Soc Econ Geologists Spec Publ 9:65–92

Anderson MR, Rankin AH, Spiro B (1992) Fluid mixing in the generation of mesothermal gold mineralisation in the Transvaal Sequence, Transvaal, South Africa. Eur J Mineral 4:933–948

Armstrong RA (2003) A geochronological investigation of the Morila gold mine, Mali. Canberra, Australian National Univ Research School Earth Sci, Precise Radiogenic Isotope Services (PRISE), p 25

Bassot JP, Dommanget A (1986) Mise en évidence d'un accident majeur affectant le Protérozoïque inférieur des confins sénégalo-maliens. Comptes Rendus Acad Sciences 302:1101–1106

Berge J (2011) Paleoproterozoic, turbidite-hosted, gold deposits of the Ashanti gold belt (Ghana, West Africa): comparative analysis of turbidite-hosted gold deposits and an updated genetic model. Ore Geol Rev 39:91–100

Béziat D, Dubois M, Debat P, Nikiéma S, Salvi S, Tollon F (2008) Gold metallogeny in the Birimian craton of Burkina Faso (West Africa). J African Earth Sci 50:215–233

Bierlein FP, Crowe DE (2000) Phanerzoic orogenic lode gold deposits. Rev Econ Geol 13:103–139

Boher M, Abouchami W, Michard A, Albarede F, Arndt NT (1992) Crustal growth in West Africa at 2.1 Ga. J Geophys Res 97(B):345–369

Boltrukevitch BN (1973) Notice explicative sur la carte des gisements et indices aurifères de la République du Mali. Unpubl Rep, SONAREM, Kati

Brooner G, Chauvel JJ, Trilboulet C (1990) Geochemistry and knowledge of banded-iron formations in the West African shield, an example. In: Chauvel JJ, Yuqi CH, El Shazly EM, Gross GA, Laajoki K, Markov MS, Rai KL, Stulchikov VA, Augusthithis SS

(eds) Ancient banded iron-formations (regional presentations). Theophrastus, Athens, p 462

Coulibaly Y, Boiron MC, Cathelineau M, Kouamelan AN (2008) Fluid immiscibility and gold deposition in the Birimian quartz veins of the Angovia deposit (Yaouré, Ivory Coast). J African Earth Sci 50:234–254

Diarra H, Holliday J (2014) Deep potential starts to emerge: new projects in Mali highlight deeper potential of Birimian belt. Mining Jour Nov 2014, 19–21

Dommanget A, Milési JP, Diallo M (1993) The Loulo gold and tourmaline-bearing deposit. Mineral Deposita 28:253–263

Feybesse J, Billa M, Guerrot C, Duguey E, Lescuyer J, Milési JP, Bouchot V (2006) The Paleoproterozoic Ghanaian province: geodynamic model and ore controls, including regional stress modelling. Precam Res 149:149–196

Fouillac AM, Dommanget A, Milési JP (1993) A carbon, oxygen, hydrogen and sulfur isotopic study of the gold mineralization at Loulo, Mali. Chem Geol 106:47–62

Gaboury D (2013) Does gold in orogenic deposits come from pyrite in deeply buried carbon-rich sediments? Insight from volatiles in fluid inclusions. Geology 41:1207–1210

Groves DI, Barley ME, Barnicoat AC, CassidY KF, Fare RJ, Hagemann SG, Ho SE, Hronsky JMA, Mikucki EJ, Mueller AG, McNaughton NJ, Perring CS, Ridley JR, Vearncombe JR (1992) Sub-greenschist to granulite-hosted Archean lode-gold deposits of the Yilgarn craton: a depositional continuum from deep sourced hydrothermal fluids in crustal-scale plumbing systems. Univer Western Australia Spec Publ 22:325–338

Groves DI, Goldfarb RJ, Gebre-Mariam M, Hagemann SG, Robert F (1998) Orogenic gold deposits: a proposed classification in the context of their crustal distribution and relationship to other gold deposit types. Ore Geol Rev 13:7–27

Groves DI, Goldfarb RJ, Knox-Robinson CM, Ojala J, Gardoll S, Yun GY, Holyland P (2000) Late-kinematic timing of orogenic gold deposits and significance for computer-based exploration techniques with emphasis on the Yilgarn Block, Western Australia. Ore Geol Rev 17:1–38

Hart CJR (2007) Reduced intrusion-related gold systems. In: Goodfellow WD (ed) Mineral deposits of Canada: a synthesis of major deposit types, district metallogeny, the evolution of geological provinces, and exploration methods. Geol Assoc Canada, Min Deposits Div, Spec Publ No. 5, pp 95–112

Hammond NQ, Robb L, Foya S, Ishiyama D (2011) Mineralogical, fluid inclusion and stable isotope characteristics of Birimian orogenic gold mineralization at the Morila mine, Mali, West Africa. Ore Geol Rev 39:218–229

Hanssen E, Kaisin J, Tessougue S (2004) The Yatela gold mine, western Mali: supergene enrichment of Lower Proterozoic gold mineralization in a surficial karst. CIM Ann Mtg, Edmonton, Conference Proceed

IAMGOLD Corporation (2014) Annual report. www.iamgold.com

Kadio E, Coulibaly ME, Kouamelan AN, Pothin KBK (2010) On the occurrence of gold mineralizations in southeastern Ivory Coast. Jour African Earth Sci 57:423–430

King K (2012) Geological, structural and mineralogical constraints on the evolution of the Morila gold deposit, south Mali, West Africa. Unpubl MSc Thesis, Kingston Univer, London, UK 170 pp

Klemd R, Ott S (1997) Compositional characteristics of fluid inclusions as exploration tool for Au-mineralization at Larafella, Burkina Faso. Jour Geochem Expl 59:251–258

Klemd R, Hünken U, Olesch M (1996) Fluid composition and source of Early Proterozoic lode gold deposits of the Birimian volcanic belt, West Africa. Intern Geol Rev 38:22–32

Klemd R, Oberthür T, Ouedrago A (1997) Gold-telluride mineralisation in the Birimian at Diabatou, Burkina Faso. J Afr Earth Sci 24:227–239

Kusnir I (1999) Gold in Mali. Acta Montan Slovaca 4:311–318

Lambert-Smith JS (2014) The geology, structure and metallogenesis of the world class Loulo-Bambadji Au district in Mali and Senegal, West Africa. Unpubl PhD Thesis, Kingston Univ, London, UK, 346 pp

Lang JR, Baker T (2001) Intrusion-related gold systems: the present level of understanding. Mineral Deposita 36:477–489

Large RR, Bull SW, Maslennikov VV (2011) A carbonaceous sedimentary source-rock model for Carlin-type and orogenic gold deposits. Econ Geol 106:331–358

Lawrence DM, Treloar PJ, Rankin AH, Harbidge P, Holliday J (2013a) The geology and mineralogy of the Loulo mining district, Mali, West Africa: evidence for two distinct styles of orogenic gold mineralization. Econ Geol 108:199–227

Lawrence DM, Treloar PJ, Rankin AH, Boyce A, Harbidge P (2013b) A fluid inclusion and stable isotope study at the Loulo mining district, Mali, West Africa: implications for multifluid sources in the generation of orogenic gold deposits. Econ Geol 108:229–257

Ledru P, Pons J, Milési JP, Feybesse JL, Johan V (1991) Transcurrent tectonics and polycyclic evolution in the Lower Proterozoic of Senegal-Mali. Precam Res 50:337–354

Liégeois JP, Claessens W, Camara D, Klerkx J (1991) Short-lived Eburnian orogeny in southern Mali: geology, tectonics, U-Pb and Rb-Sr geochronology. Precam Res 50:111–136

Masurel Q, Thébaud T, Miller J, Ulrich S, Hein KAA, Cameron G, Beziat D, Bruguier O (in press) Sadiola Hill: a world-class carbonate-hosted gold deposit in the Birimian terranes of Mali, West Africa. Econ Geol

McCuaig TC, Kerrich R (1998) P-T-t-deformation-fluid characteristics of lode gold deposits: evidence from alteration systematics. Ore Geol Rev 12:381–453

McCuaig TC, Kerrich R, Groves DI, Archer N (1993) The nature and dimension of regional and local gold-related hydrothermal alteration in tholeiitic metabasalts in the Norsemann goldfields: the missing link in a crustal continuum of gold deposits. Mineral Deposita 28:420–435

McFarlane C, Mavrogenes J, Lentz D, King K, Allibone A, Holcombe R (2011) Geology and intrusion-related affinity of the Morila gold mine, southeast Mali. Econ Geol 106:727–750

Meinert LD, Dipple GM, Nicolescu S (2005) World skarn deposits. Economic Geology 100th Ann Vol 299–335

Milési JP, Feybesse JL, Ledru P, Dommanget A, Ouedrago M, Marcoux E, Prost A, Vinchon C, Sylvain JP, Johan V, Tegyey M, Calvez JY, Lagny P (1989) West African gold deposits in their Lower Proterozoic lithostructural setting. Chron Recherche Minière 497:3–98

Milési JP, Ledru P, Feybesse J, Dommanget A, Marcoux E (1992) Early Proterozoic ore deposits and tectonics of the Birimian orogenic belt, West Africa. Precam Res 58:305–344

Oberthür T, Vetter U, Schmidt Mumm A, Weiser T, Amanor JA, Gyapong WA, Kumi R, Bleckinsop TG (1994) The Ashanti gold mine at Obuasi in Ghana. Geolog Jahrbuch D100:31–129

Ohmoto H, Goldhaber MB (1997) Sulphur and carbon isotopes. In: Barnes HL (ed) Geochemistry of hydrothermal ore deposits, 3rd edn. Willey, New York, pp 517–612

Olson SF, Diakite K, Ott L, Guindo A, Ford CRB, Winer N, Hanssen E, Lay N, Bradley R, Pohl D (1992) Regional setting, structure, and descriptive geology of the Middle Proterozoic Syama gold deposit, Mali, West Africa. Econ Geol 87:310–331

Ouattara Z, Coulibaly Y, Boiron MC, Lieben F (2014) Geology and ore localizations in the Bonikro gold deposit, Fettékro greenstone belt, Côte d'Ivoire. Soc Economic Geologists Keystone Conference, Abstracts

Phillips GN, Powell R (2010) Formation of gold deposits: a metamorphic devolatilization model. J Metamorph Geol 28:689–718

Quick R (1999) The Morila gold deposit, southern Mali, West Africa. Unpubl MSc Thesis, Leicester University, Leicester, UK

Randgold Resources Ltd (2014) Annual report. www.randgoldresources.com

Ridley JR, Diamond LW (2000) Fluid chemistry of orogenic lode gold deposits and implications for genetic models. Rev Econ Geol 13:141–162

Schidlowski M, Hayes JM, Kaplan IR (1983) Isotopic inferences of ancient biochemistries: carbon, sulphur, hydrogen and nitrogen. In: Schopf JW (ed) Earth's earliest biosphere: it's origin and evolution. Princeton University Press, New York, pp 149–186

Schmidt Mumm A, Oberthür T, Vetter U (1997) High CO_2 content of fluid inclusions in gold mineralizations in the Ashanti belt, Ghana: a new category of ore forming fluids. Mineral Deposita 32:107–118

Sillitoe RH, Thompson JFH (1998) Intrusion-related vein gold deposits: types, tectono-magmatic settings and the difficulties in distinction from orogenic gold deposits. Resour Geol 48:237–250

Smith DS (1996) Hydrothermal alteration at the Mineral Hill mine, Jardine, Montana; a lower amphibolite facies Archean lode gold deposit of probable syn-metamorphic origin. Econ Geol 91:723–750

Tomkins AG (2010) Windows of metamorphic sulfur liberation in the crust: implications for gold deposit genesis. Geochim Cosmochim Acta 74:3246–3259

Treloar PJ, Lawrence DM, Senghor D, Boyce A, Harbidge P (2014a) The Massawa gold deposit, eastern Senegal, West Africa: an orogenic gold deposit sourced from magmatically derived fluids? Geol Soc Spec Publ 393:135–160

Treloar PJ, Lawrence DM, Lambert-Smith J, Senghor D, Wiedenbeck M, Boyce A (2014b) West African orogenic gold deposits: do they fit the global paradigm? IMA 2014 Conference Johannesburg, Abstract Vol

Villeneuve M, Cornée JJ (1994) Structure, evolution and paleoceanography of the West African craton and bordering belts during the Neoproterozoic. Precam Res 69:307–326